Biophysical Chemistry 5 (1976) 77–96


# MaD, AN AUTOMATED PRECISE ANALYTICAL ULTRACENTRIFUGE SCANNER SYSTEM*

René COHEN, Jean CLUZEL, Henri COHEN**, Philippe MALE‡, Max MOIGNIER and Claude SOULIE
*Institut de Biologie Moléculaire, – C.N.R.S., Paris VII, 2 place Jussieu, 75005 Paris, France*

The various hardware components of this scanning system, a mechanical split-beam scanner with its photomultiplier measuring slit, minimum analog electronics and an important digital part (computer, interface), are intimately interwoven by an elaborate software. A high degree of automation and sophistication is thus reached. On the one hand, all the photoelectrons coming from each light pulse are integrated. The result, after conversion to digital form enters the computer; a high precision is thus reached: $10^{-5}$ absorbance unit (A.U.) under very favorable conditions, and $10^{-4}$ A.U. for conventional sedimentation studies. On the other hand, during its motion along the image, the precise slit position is permanently known by the system: the sector image is thus segmented into precisely defined zones, inside which the average absorbancies are determined, punched, plotted and printed. New and very useful utilizations and improvements of analytical ultracentrifugation are now possible: the fixed radius mode, permits precise $s$ determination by following the radial dilution; $s$ can be precisely measured by time difference curves even when the solution absorbancy is comparable to the base line variations (0.01 A.U.); round trip analyses permit very long analyses without the absorbancies distributions distorsions due to very long one-way scans during sedimentations runs; reductions of the effect of the stray light by a factor of ten. This system has been in routine use for four years.

## 1. Introduction

An entirely novel split-beam photoelectric scanner system for the absorption optics of an analytical ultracentrifuge [1] is described in this paper. It has been in routine use since the fall of 1971. Except for minor details in the presentation of results, the system has not been changed. This system arose from active enzyme centrifugation experiments performed on crude cell extracts. The specific enzymatic activities are very low in such extracts, the measured absorbancies often being smaller than 0.01 absorbancy unit. This latter value corresponds to the noise of the commercial scanner or of the photographic technique. Thus an entirely new system had to be devised.

The principles on which its construction rests, as well as preliminary results, have already been published in a French written grant report [2]. A US patent, applied for in 1971, was granted in 1973 [3]. Since then, other scanners have been described (a bibliography will be found in [4]; some are also described in the present issue devoted to the fiftieth anniversary of the analytical ultracentrifuge).

Thus, it seems important to present now a full description of this system as well as a full report on the results obtained with it. This will be done in a series of papers.

In what follows we assume the reader to be familiar with the recent exhaustive Schachman and Edelstein review article [4] to which in this paper, explicitly or implicitly reference is often made.

The system described here includes a mechanical scanning device, M, minimum analog electronics, a, and a very important digital part, D, (computer, interface, plotter), thence its name MaD.

The scanner which is part of MaD is, in a way, a typical Schachman type split-beam scanner [5], i.e. it works with the absorption optics of the centrifuge, it

* The preliminary study of the system was made possible by a special C.N.R.S. grant (RCP. 148, 1967–1969). The construction of MaD was supported by the D.G.R.S.T. (Comité de Génie Biologique et Médical, grant 68-01-307, 1968–1970).
** Present address: UER de mathématiques et informatique, Université de Bordeaux 1, 33405. Talence, France.
‡ Present address: Cell. Biology, Yale University, 333 Cedar Street, New-Haven, Connecticut 06510, USA

makes use of double-sector cells, it receives the light pulses (through an adjustable slit) on a photomultiplier (PM) cathode, the slit scans the cell image mechanically, its motion along this image being related to the rotation of a coded disk. Also, as in a later version of the Schachman scanner [6], it makes use of the light coming from the rotor references hole through the Schlieren optics. But, the signals coming form the PM, from the coded disk or from the reference hole, are treated in a way radically different from any other scanner.

The system's true nickname should be MaDS because it includes very important software which is an inherent part of the system. This software is required throughout, at every fraction of each light pulse, for moving the measuring PM slit, etc. The interface hardware and the software were developed simultaneously, and during the construction we often had to decide which part of the task should be given to the software and which to the hardware. Consequentiy, there is some unusual phrasing in this paper where MaD is often considered as a thinking and decision making creature.

After showing how we fulfilled the conditions we through were necessary for a scanner to take full advantage of the centrifuge absorption optics and to be as precise and as automated as possible, a brief physical description will be given. This will be followed by a detailed explanation of the ways software and hardware intermingle during centrifugation. The communication between the experimenter and MaD will then demonstrate the system versatility. Some unusual results will be summarized and finally two conventional sedimentation runs will show the sensitivity of the system. Details will be given in forthcoming papers.

## 2. The a priori conditions

### *2.1. Condition one*

To measure a light pulse with the highest possible precision, one must integrate the whole corresponding signal coming from the PM. This is very important in the case of the centrifuge absorption optics where the number of photoelectrons per pulse can be smaller than 100. In order not to loose any fraction of any pulse, we have to generate electronic gates at very pre-

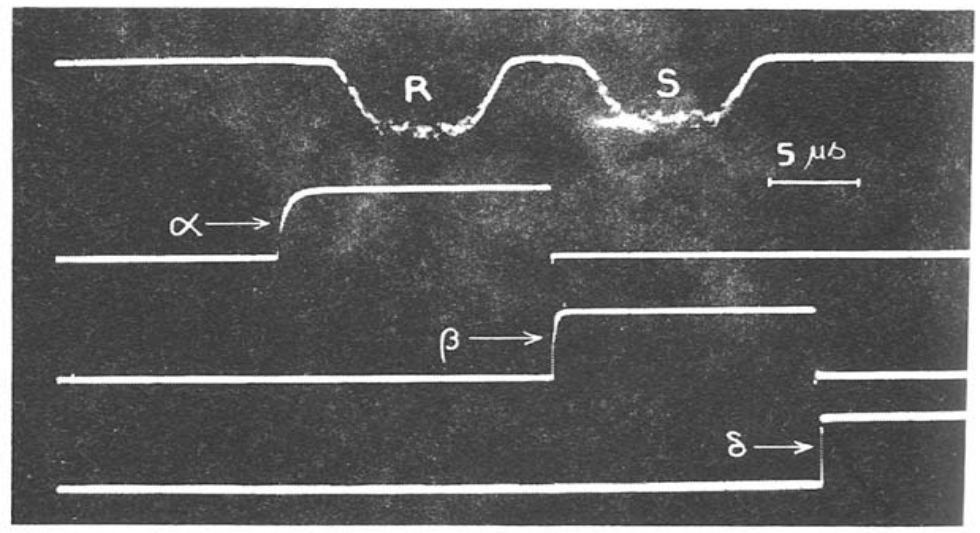


Fig. 1. Photograph of a four-channel oscilloscope screen, taken during a typical run of MaD. This shows the time relationships between the R and S pulses and the three gates $\alpha$, $\beta$ and $\delta$. Centrifuge speed: 56,000 rpm, double sector (2.5°) cell, wavelength 365 nm. One can observe the light source intensity fluctuations (R and S pulses) and the constancy of the time relationships during the almost 100 revolutions which occurred during the 0.1 second exposure. Each gate is generated at the beginning of the sharp voltage rise of its corresponding circuit (the differences between the rise times of the three gates are due to minor differences between their circuits). Normally, we use a two channel oscilloscope triggered by the $\alpha$ gate and showing the $R$ and $S$ pulses. The $\beta$ gate coincides with the end of the $\alpha$ signal and is thus also visible.

cise moments (just before and just after each pulse). For example, for a double sector cell, a first gate, $\alpha$, should connect the PM with a convenient measuring device (an integrator in our case) just before the beginning of the signal corresponding to the first sector. A second gate, $\beta$, is needed in the middle of the very short "dark" stage between the signals corresponding to the two sectors. This gate $\beta$ has a double role: it cuts the connection between the PM and the measuring device, and connects simultaneously the PM to a second such device. A third gate, $\delta$, just after the end of the signal corresponding to the second sector, cuts the connection between the PM and the second device (fig. 1).

The dark stage lasts about $2 \times 10^{-3}\ T$ ($T$ = period = duration of a rotor revolution); thus the error in the time at which the $\beta$ gate should be generated, must be smaller than $\pm 3 \times 10^{-4}\ T$. This precision precludes any permanent setting of $\beta$ since any slight centrifuge speed variation could throw $\beta$ out of the dark period.

For many reasons, it is practically impossible to use optical methods (inside the centrifuge chamber)

for generating the gates at the right times and with the required precision. Only a digital computer is suitable for this; but, even a computer is not enough. Indeed, although it easily measures the time $T$ with a relative error of $10^{-4}$, it would be unable, by itself, to generate, at each revolution, gates with the needed precision. Thus, at 68,000 rpm, where $T = 882\ \mu s$, $\beta$ should be generated with a precision of $\pm 0.25\ \mu s$ which is impossible, even now in 1975, for any normal computer.

So an interface between the centrifuge and the computer had to be used; it has been built around a 5 MHz clock giving pulses every 0.2 $\mu$s. A 16 bits, 0.96 $\mu$s cycle time computer was used. A 4 K core memory was sufficient, but the addition of a second 4 K core memory (in 1971) improved vastly the dialogue with MaD and the presentation of the results on the plotter. The measuring devices were operational amplifiers used as integrators. An other possibility, the photon counter, is discussed in section 7. How the gates are generated will be explained in section 4.1.

### *2.2. Condition two*

As soon as the integration is complete, it is mandatory to shelter its results from all electronic noise in such a way as not to spoil the precision obtained through the application of condition one (fig. 2).

Since the system already includes a computer, we then fulfilled this condition by using a classical solution: an analog to digital converter (ADC), 12 bits, 8 $\mu$s conversion time, connected to the computer. In practice, the conversion starts immediately on completion of the integration. It is only in the case of double sector cells and at the highest centrifuge speeds that the conversion of the second sector cannot start immediately. In the worst case (68000 rpm) the hold time is smaller than 8 $\mu$s.

As will be shown later the final absorbancy values are calculated averages corresponding to many revolutions (always more than at least 6 to 8, often more than 100 and sometimes up to 30.000). This allowed us to invert the role of the two integrators at each revolution in such a fashion that the signal coming from each sector is alternatively routed to the first and then to the second integrator. In other words, from the cell image to the computer, the reference sector, R, and the sample sector, S, are treated identically by the same PM, the "same" integrator, the same ADC, and the two converted values enter the computer by interruption through the same line.

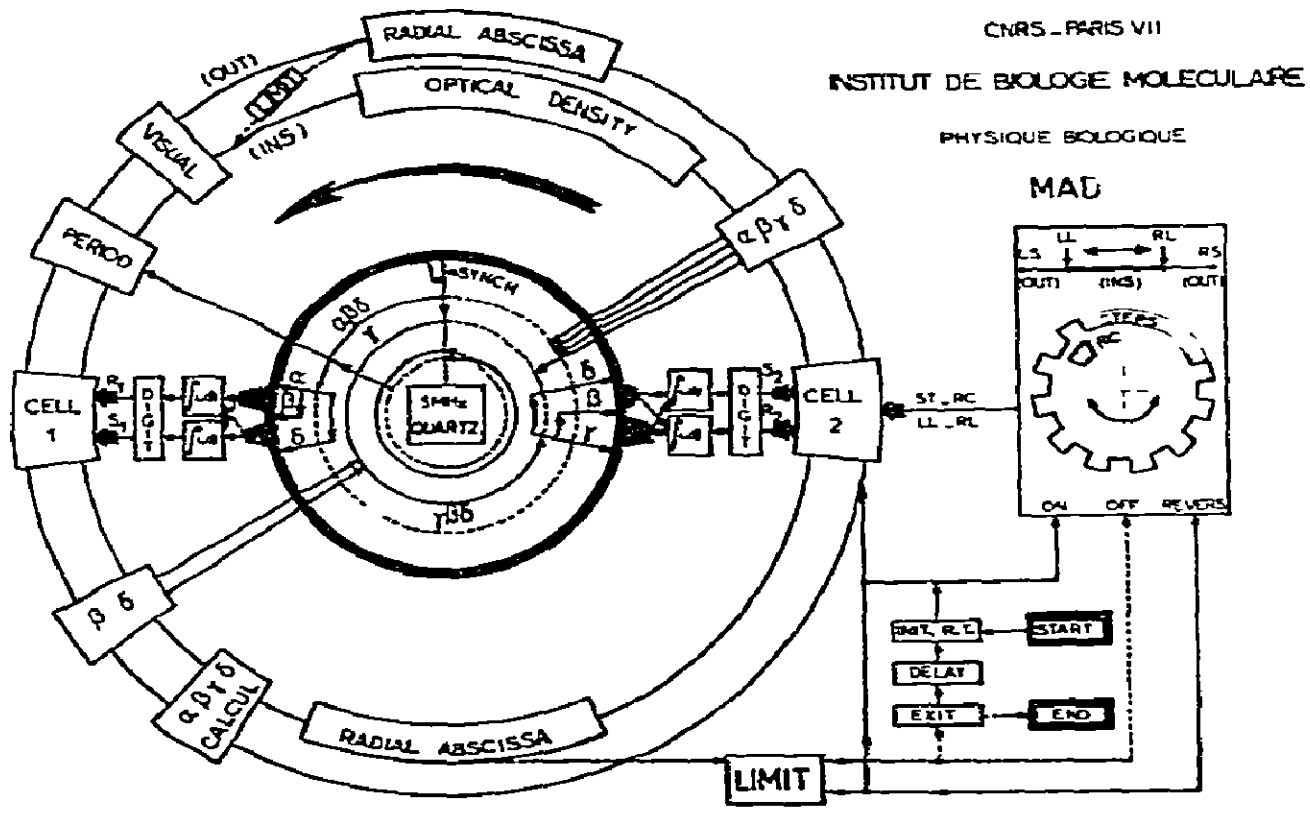


Fig. 2. MaD organigram. DIGIT represents the analog to digital converter. In the interface (inside the thick circle), full circles represent registers counting down the pulses, delivered every 0.2 $\mu$s, by the 5 MHz quartz oscillator circuit, while the dotted circles correspond to standing registers. For other details, see sections 2 and 4.

It turned out that fulfilling conditions one and two reduced to a very low level the magnitude of the electronic noise coming from the gates and from the only three operational amplifiers used (PM high speed buffer, integrator amplifier and analog part of the ADC) and integrated during the short duration of a pulse. What is of paramount importance is that it rendered the noise very constant. We could, if necessary, adjust the amplifiers bias offsets and get almost zero average noise values; but these values depend on the PM voltage and on the integrators time constants. Instead, when a high precision is required, we prefer to use the method explained below in the section describing condition three. Although we almost never do it, we could also give the value of the average noise as an answer to the question number 12 asked by the teletype at the beginning of the experiment (section 5); this value would then be substracted automatically from the experimentally measured values before any absorbancy calculation.

### 2.3. Condition three

The system should be able to measure during each rotor revolution the four values corresponding to two double sector cells situated 180° apart.

Before explaining the reasons for this principle, it should be pointed out that "multiplexing" in MaD is simply performed by putting into the program, once and for all, the 2, 4 or 6 values needed for the description of the mechanically defined angular positions of the holes of any multicell rotor. The system then scans in sequence the different cells, the computer generating for each cell the $\alpha$, $\beta$ and $\delta$ gates at the right times for the corresponding hole. The reason behind principle three is the necessity of subtracting from the measured values any electronic noise as well as the effect of the stray light. It is well known that the light "turning around" the rotor or coming from the other than the measured sector represents about 3% of the light coming through a non-absorbing sector. It is therefore very dangerous to measure absorbancies greater than one; until now the limiting observed value in the case of an infinitely absorbing samples was thus close to 1.5. In order to apply principle three, other gates are needed for a second cell. Without contrary instructions, MaD assumes the two cells to be 180° apart and these three new required gates are generated exactly half a revolution after the three corresponding gates of the first cell (fig. 2).

When the four pulse values corresponding to the same revolution are measured and are handled arithmetically by a digital computer, it is easy to increase the workable absorbancy range up to about 2.2, the limiting observed absorbancy now reaching a value close to 2.8. This is simply done by filling the first cell normally (R1 buffer, S1 sample) and filling the R2 sector (opposite to R1) of the second cell with the same buffer as R1, while S2 is filled with a solution opaque to the wavelength used (absorbancy $\geqslant 4$). After each revolution, the computer then calculates the absorbancy as $\log([R1-S2]/[S1-S2])$ instead of the usual $\log(R1/S1)$. In other words, we do not diminish the stray light, or the electronic noise, but we reduce their effects by at least a factor of ten.

It should be pointed out that the simultaneous precise measurements of four sectors allows other types of experiments. For example, one can measure two double sector cells simultaneously for differential measurements.

### 2.4. Condition four

A real automated system requires that the true radial positions corresponding to the PM slit position along the cell image, should always be known during the scan. It should be possible for example, to scan any limited domain (defined by its two extreme radial positions), even when at the start the PM slit is at any unknown position along the cell image. This condition is also necessary for performing round-trips (cf. condition five).

In the application of this principle, use has been made of a disk (fig. 2) which, as in the Schachman scanner, is coaxial with the screw which moves the PM and is rigidly fastened to this screw. Along the edge of the disk are 48 steps, 24 full, 24 empty; with the help of a small light source and of a photodetector connected to an amplifier, the logical status of the amplifier output alternates between 0 and 1 while the disk rotates, the rotation angle for each status being equal to $360°/48 = 7.5°$. Since the screw pitch is 1.500 mm, one step (empty or full) corresponds to $1.500/48 = 31.25\ \mu$ along the cell image (i.e. roughly to 15 $\mu$ at the cell). The status 0 or 1 corresponding to these steps is always available at the computer input;

it will be called the step bit (ST). On the same disk but at smaller radius than the steps a special aperture, the revolution counter, 13° wide, with a similar optical device gives rise to the RC bit whose value is normally 0 and is 1 only when the light can reach the detector.

Two other simple light source–detector devices to which correspond two bits, the left stop (LS) bit and the right stop (RS) bit are fixed to the scanner itself. They are positioned in such a way that:
(1) according to the PM slit position along the cell image, these two bits have the status given in fig. 3, on which the RC and ST bits values have been also represented, in their exact angular relationship and
(2) the domain between the two stops encompasses the cell and rotor hole image corresponding to the highest optical magnification ever used in the absorption optics. It corresponds to 24 screw revolutions, i.e. to 36 mm. The cell top is towards the left stop.

The RC aperture has been cut in order to be 13° wide and to symmetrically encompass two contiguous 7.5° steps. On the other hand the left and right optical stops positions have been adjusted and permanently fixed so as to cause their corresponding bit change to occur somewhere in the middle of periods during which the RC bit is zero.

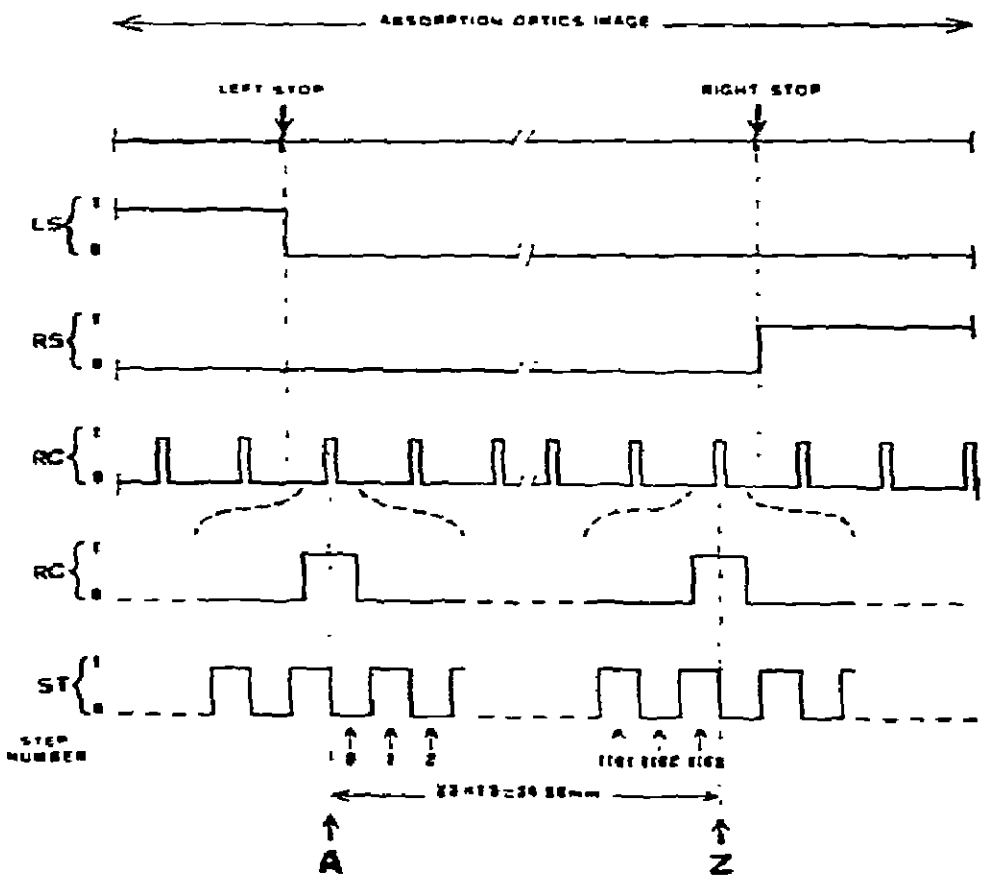


Fig. 3. Determination of the slit position along the cell image. The time scale is expanded for the RC and the ST bits. The coded disk and the light-detector assembly of the ST bit have been adjusted so as to equalize the rotation angles (7.5°) corresponding to its two status, conditions, 0 and 1. For other details, see text section 4.3.

The RC, LS and RS bits as well as the ST bit status are always available at the computer input; it is then clear that once the PM slit crossed the left (or the right) stop, MaD is able to recognize precisely the slit position at any further time (cf. subsection 4.3).

### 2.5. *Condition five*

The absorbancy distributions given by the system should be as close as possible to the ideal undeformed distributions which would be obtained if the scans were instantaneous.

Deformations arise from the fact that different regions of the cell image are measured at different times. As long as only equilibria are studied or maxima positions looked at, either there is no deformation or if any is present it can be easily corrected. Since, as will be shown below in the results section, the accuracy depends only on the total amount of light received by the PM slit, very long scans were contemplated, for example (velocity sedimentation) four minutes in every five. The deformations arising from such a long one-way scan would not have allowed any serious analysis of the distributions detailed structures.

We then use the round-trip analysis: the absorbancies measured both ways at the same radial position are averaged and it can be shown that the averaged distribution thus obtained is very close to the instantaneous distribution at the middle of the round trip, i.e. at the time the PM slit reverses its motion [14]. Since MaD always knows where the PM slit is, the round trips are easily performed, the only problem being the backlash of the screw which moves the PM slit. Due to this effect, the same position along the cell image corresponds to steps which have different numbers for the two opposite scans of the round trip. This problem was easily solved by the initial round trip (cf. subsection 4.4) during which the system itself measures this backlash and takes its value into account in the step enumeration.

### 2.6. *Condition six*

To avoid any ambiguity in the presentation of the

data and in the plotting and the use of "curves", with the associated problems of interpolation and of sampling, the results should be given as true calculated averages on very precisely defined abscissae zones (figs. 5, 8, 9 and 11).

MaD segments the radial distribution of absorbancies along the studied domain of the cell in contiguous and rigorously equal radial zones and gives the calculated average absorbancies in each of these zones. The common width of these zones is chosen by the experimenter. It corresponds to an integer number, $n$, of steps of the coded disk, i.e., each zone corresponds to $31.25 \times n$ microns at the cell image (usually $n \geqslant 2$). The number of zones is usually chosen smaller than 500.

Since MaD always knows where the PM slit is during its motion along the cell image, it knows exactly when the slit enters the $j$th zone and when it leaves it. Many rotor revolutions occur during this time interval. For each of them, the absorbancy is calculated and at the end of the time interval, all these values are averaged and put in the memory corresponding to the $j$th zone. If a one-way scan has been asked for, this value will be given at the end of the analysis. If a round trip is done, the average absorbancy corresponding to the same zone on the way back will be added into the same memory and the two values averaged.

In the next paper of this series, the effect of the above adopted zoning (or grouping) on the true absorbancies radial distributions will be discussed at length.

It suffices to recall here that when a true gaussian curve is measured stepwise in zones of width $l$ [7] or by a sliding slit of width $l$ [8], one has

$$\sigma^*/\sigma \simeq 1 + k(l/\sigma)^2,$$

where $\sigma$ is the true gaussian standard deviation, $\sigma^*$ the observed one of the quasi-gaussian curve resulting from the measurements and $k$ a constant close to 0.042. Thus when a 100 $\mu$ slit is used, there is already a widening and a 31 $\mu$ grouping has the same effect as using a slit only 5% wider [indeed $(100^2 + 31^2)^{1/2} = 105$].

The absorbancies are calculated with a precision of $10^{-6}$ absorbancy units, but clearly it is only when they correspond to averages made over a great number of rotor revolutions that more than four decimal figures are meaningful. The digital plotter is programmed to allot exactly one millimeter per zone (horizontal axis); the value in each zone is represented as a horizontal (1 mm long) segment connected by a vertical line to the value of the next zone. The results, once plotted, appear in the shape of a histogram which represents exactly what has been measured on both axes. Radial abscissae increase always towards the right.

The 30 cm of the vertical axis are used in the following fashion (fig. 11): the central 20 cm always correspond to an absorbancy range fixed by the experimenter (for example from −0.017 to +0.003), the upper 5 cm correspond to the range +0.003 (in the above example) to +3.0 (always) and the lower 5 cm correspond to −0.017 (in the above example) down to −3.0 (always). The corresponding scales are printed at the end of the last analysis.

On the other (radial abscissa) axis a small circle representing the reference hole is marked at the position determined by the initial round trip. For the initial round trip, and for it only, the results are plotted differently, as described in section 4.4. The absorbancies can also be punched (paper tape) and printed.

### 2.7. Condition seven

All the important data should be easily and instantaneously displayed. A two-channel oscilloscope triggered by the $\alpha$ gates shows the $\beta$ gates and also the R and S pulses and thus displays clearly and permanently the time relationship between pulses and gates (fig. 1). By the 16 combinations of four keys, it is possible to visualize at will on the computer console almost any relevant instantaneous information (as 16 lighted-bits words):

(1) the values of the period, of the R1, S1, R2, S2 pulses, of R1 − S2 and of S1 − S2, if these values should enter the absorbancies calculations, etc.;

(2) the status of the ST, RC, LS and RS bits as well as the step number and the zone number in which is the PM slit;

(3) the screw motor direction, the number of scans and of analysis already performed during the current experiment, etc.

These two displays are very useful indeed and without the console display it would have been very difficult to tune the whole system.

## 3. Brief physical description of MaD

Only the main differences from the other scanners will be described. The centrifuge is a Beckman Spinco model E, equipped with a monochromator.

### *3.1. The mechanical part (built entirely in this laboratory)*

The cell image can be sent from the always functional photographic camera to the horizontal plane of the scanner through a 45° mirror. A switch permits removal of the mirror from the optical path, returning the image to the camera. The system has been adjusted permanently for the two systems to be simultaneously in focus (actually we almost never use the photographic system except for checking its correct focusing).

The PM housing is moved by a motorized 1.50 mm pitch screw. The duration of a full length one way scan (36 mm) can vary continuously from 2.5 to 500 seconds; it is under the control of two independent potentiometers, hand-set before a run by the experimenter. One (usually corresponding to a fast motion) is used by MaD to bring the slit to the image domain which has to be studied; the other is used when the absorbancies measurements are being made. The shift orders are given at the right times by MaD (cf. subsection 4.3). A clutch permits the experimenter to free the PM from the screw rotation; this is very useful when experimental conditions have to be changed (optical magnification, scan speed, slit dimensions, etc.). The PM housing also carries the adjustable measuring slit. Two micrometers can vary continuously its two dimensions from 0.00 to 5.00 mm.

### *3.2. The scanning photomultiplier*

Except when orange and red light is needed, an EMI 13 dynode 6256 S photomultiplier is used. The values for 11 decoupling capacitors were very carefully calculated, since it was essential for the PM gain to recover at least 0.9997 of its initial value at the beginning of the second pulse when a double sector cell was spinning at more than 60,000 rpm! At the beginning of an experiment, the high voltage value is fixed (cf. subsection 4.4). According to the manufacturer, the high voltage is stabilized to 0.001% which corresponds to a gain stability close to 0.01%.

### *3.3. The SYNCH pulse photomultiplier*

We use a 1P28 photomultiplier fastened on top of the Schlieren plate holder which receives by means of a fixed 4 mm by 4 mm, 45° mirror and a conveniently oriented very narrow slit, the light corresponding to the rotor reference hole in the Schlieren optical beam.

The light pulse is treated as giving a logic pulse (SYNCH) at a time always corresponding to the same rotor azimuth (to ± 0.1°). We constructed the electronics so as to make this angle relationship independent of the long term decrease of the intensity of the dc filament light source which we use (its housing can rotate from an out of the way position to its working position atop the regular Schlieren source).

### *3.4. The computer*

A DDP (now H) 516 Honeywell computer with a 0.96 μs cycle time was used. It has 8 K words of 16 bits, a fast arithmetic option, a teletype, a fast paper tape reader and a fast paper tape punch. There are no magnetic tapes nor disks. The very complex and elaborate interface with the analytical ultracentrifuge has been conceived and built in the laboratory, as well as the very simple interface with the Benson digital plotter.

## 4. Detailed description of an experiment

### *4.1. Gate generation during a rotor revolution (fig. 2)*

The concentric circles show what happens during every rotor revolution. The two outside circles represent the various subprograms and the order in which they are executed. The thick circle shows, on its outer side, the light pulse coming from the photomultiplier situated at a fixed position on the image of the Schlieren optics and its corresponding SYNCH pulse and on its inner side, the four signals given by the scanning photomultiplier slit and corresponding to two double sector cells. Inside is the interface whose heart is a 5 MHz quartz oscillator, thus giving the required 0.2 μs accuracy.

The first double circle around the quartz oscillator represents a register which will measure the period, i.e. will count the number of quartz oscillator pulses during one rotor revolution. A SYNCH pulse starts the counting by this register (previously reset to zero); at the next SYNCH the counting is stopped and the register now contains the period. At this point, the computer asks for this period and inputs its value and the register is then reset to zero. The period is asked for at every revolution but every other revolution the answer is "not ready" (the register is counting) and the PERIOD subprogram makes use of the previous value. Later the $\alpha\beta\gamma\delta$ CALCUL subprogram calculates the times at which the gates $\alpha$, $\beta$, $\gamma$ and $\delta$ should be generated. In the calculations, the constants describing the rotor geometry as well as the variable period value are needed. The gate $\alpha$ should be generated about 86.5° after SYNCH and the gate $\gamma$ 180° later, i.e. 266.5° after SYNCH. In order to use fewer and smaller registers, thereby saving some money, the times at which the $\beta$ and $\delta$ gates should be generated are calculated from the time at which $\alpha$ (or $\gamma$) is itself generated; $\beta$ thus corresponds to 4.5° and $\delta$ to 9°; the same $\beta$ and $\delta$ registers are used by both cells. Later during the same revolution (subprogram $\alpha\beta\gamma\delta$) the computer sends to the interface the four previously calculated values, thus setting the four registers $\alpha$, $\beta$, $\gamma$ and $\delta$ to these values (for example if the speed is 60,032 rpm, the "period" is 4997; the calculated values are then $\alpha = 4997 \times 86.5/360 = 1201$, $\beta = 62$, $\gamma = 3699$ and $\delta = 124$).

When SYNCH arrives, it starts the counting down of the quartz oscillator pulses by the $\alpha$ and $\gamma$ registers (but not by $\beta$ and $\delta$). When register $\alpha$ reaches zero, the $\alpha$ gate is generated and simultaneously both registers $\beta$ and $\delta$ start to count down, giving rise to the corresponding $\beta$ and $\delta$ gates when they reach zero (cf. also fig. 1). During this time $\gamma$ is still counting down and the $\beta$ and $\delta$ registers have to be reset (for the second double sector cell) to the same values as before (in the above example, to 62 and 124); this is done by the subprogram $\beta\delta$. Finally, the three necessary $\gamma$, $\beta$ and $\delta$ gates are generated in the same manner for the second cell.

The VISUAL subprogram permits the visualization of all the important data on the computer console (cf. condition seven). It is clear that the SYNCH pulse is the deus ex machina because, at each revolution, not only does it start or stop the period measurement, and start the count down of the $\alpha$ and $\gamma$ registers but it also inverts the role of the two integrators.

### *4.2. Treatment of the light pulses*

In fig. 2, adjacent to the two pairs of signals which correspond to the light pulses coming from the two double sector cells, are represented the two integrators ($\int i\,dt$) and the analog to digital converter (DIGIT). Actually, the same pair of integrators is used for the both cells. They are reset to zero once the values they carry (R1 and S1 or R2 and S2) are converted (there is only one converter for converting these four voltage values). Once a conversion is completed, the computer is *interrupted* (in reality, the program is organized so that what it was doing previously is finished when the interruption arrives); it receives (thick arrows) the value (CELL 1 or CELL 2 subprograms) and checks if it corresponds to the right sector (the first should always come through a specific address, the second through another one). If not, the computer halts and a siren blasts (as it does when any one of the very many other controls fails).

After each revolution, four 12 bits values, R1, S1, R2, S2, are then available for absorbancies calculations (OPTICAL DENSITY). The value of the four bits ST, RC, LS and RS are always available at the computer input but they enter it, as part of a 16 bits word, along with the 12 bits of S when the latter its conversion completed, interrupts the computer. Four other useful informational bits (motor potentiometers, motor direction, and shutter status) enter the computer with R values. These 8 bits are examined by MaD only once per revolution (CELL 2 subprogram).

### *4.3. The radial positions*

Radial positions are handled by the RADIAL ABSCISSA subprogram. The PM slit should always be at the left of the left stop at the start of an analysis. If it is not there (and MaD knows it by looking at the values of the LS and RS bits), the computer gives an order to the slit to go fast to the left; the motion is stopped when MaD recognizes that the PM slit is where it should be, i.e., on the left of the left stop.

The analysis can then begin and the slit is ordered to move to the right at a speed preset by the experimenter and usually slower than the above one. MaD watches first the value of the LS bit (fig. 3); when it becomes zero, MaD watches the RC bit. Then, when it becomes equal to one, MaD waits for the ST bit to shift from 1 to 0: when this happens, MaD knows that the slit just entered step number zero, the absorbancies measurements can start, and from then on MaD will always know exactly where the PM slit is along the image. The RS bit helps to recognize step number 1103 during the initial round trip. From A to Z (fig. 3), 34.50 mm can thus be studied. Various controls on these four bits values are made and if, for any reason, the phase relationships do not seem to hold, the siren blasts.

Usually, we analyse a domain smaller than the whole image between the left and right stops. At the beginning of the experiment, the domain limits are then given in terms of step number as left limit (LL) and right limit (RL). These should correspond to a RC bit = 1 position, i.e. they should be multiples of 48; then MaD, always knowing where the PM slit is, scans only the required domain. Usually (cf. above) an analysis does not correspond to a single scan but to one or a series of round trips between the two assigned limits. MaD keeps a precise accounting of the step number and averages the absorbancies measured both ways at the same radial position (for the backlash, cf. below).

It should be noticed that because we already had a computer, this laboratory built radial abscissae coding device turned out to be cheaper, more precise and much more versatile than any commercially available coded system we know of. Note also that in order not to miss any ST bit change there should be at least one rotor revolution for a 7.5° (one step) rotation of the coded disk (since it is only once per revolution, with the S2 value, that the ST bit enters the computer). If not, two ST bit changes will be missed, the next RC bit will not be in phase with the ST count, and the siren will blast. In practice this means that in order to avoid the siren, one should not scan the entire cell image in less than 15 seconds at 6000 rpm, and less than 1.5 second a 60,000 rpm; these are very easily fulfilled conditions.

In fig. 2, the (OUT) circle represents the subprograms used by MaD when the slit is not in the domain which should be studied and thus where only the radial abscissae have to be known; the (INS) corresponds to the measuring mode. The shifts (INS) ⟷ (OUT) occur when the slit encounters the left or the right limit.

### *4.4. The initial round trip*

The purpose of the initial round trip is to identify, in terms of step numbers, the positions of the cell top, the cell bottom, the reference hole, and sometime the reference R1 sector meniscus; it also measures, again in step numbers, the PM slit screw backlash, permitting MaD to keep an exact accounting of the radial abscissae during round trip analyses. See figs. 4 and 5. Since they are known in terms of step numbers, these positions are also known in term of true distances along the cell image (since 48 steps correspond to 1.500 mm). If, furthermore, Q 16 and Q 17 (cf. section 5) or even sometimes Q 17 and Q 18 have been answered correctly, these positions are then given and printed as true radial abscissae (i.e. in cm at the cell). During an initial round trip only the R1 sector (usually filled with a non absorbing solution) is measured.

Typically, at the beginning of a run, MaD directs the PM slit to go to the left of the left stop (if it is not already there). Then, the slit begins moving to the right, until it enters (cf. above) in step number zero which always corresponds to a dark region above the sector top. As soon as the R1 signal is above a fixed threshold value, $a$, MaD knows that the slit is entering into the sector; one mm later the R1 value starts being averaged (moving average) until the instantaneously measured R1 value remains lower than 0.8 times the average. This average value, $M$, is kept in memory. Then the slit reaches the cell bottom, and R1 becomes again smaller than the threshold value, $a$. If R1 remains smaller than $a$ for more than six steps, then MaD knows that the slit is in the dark area and that what will come later is the reference hole. But, in order to be able to see the light coming from it, the gate $\alpha$ should be displaced by 90° from about 86° to 176°, this because the reference hole intercepts the absorption optics beam about half a revolution after the SYNCH pulse.

We have then, in the dark, a program change in

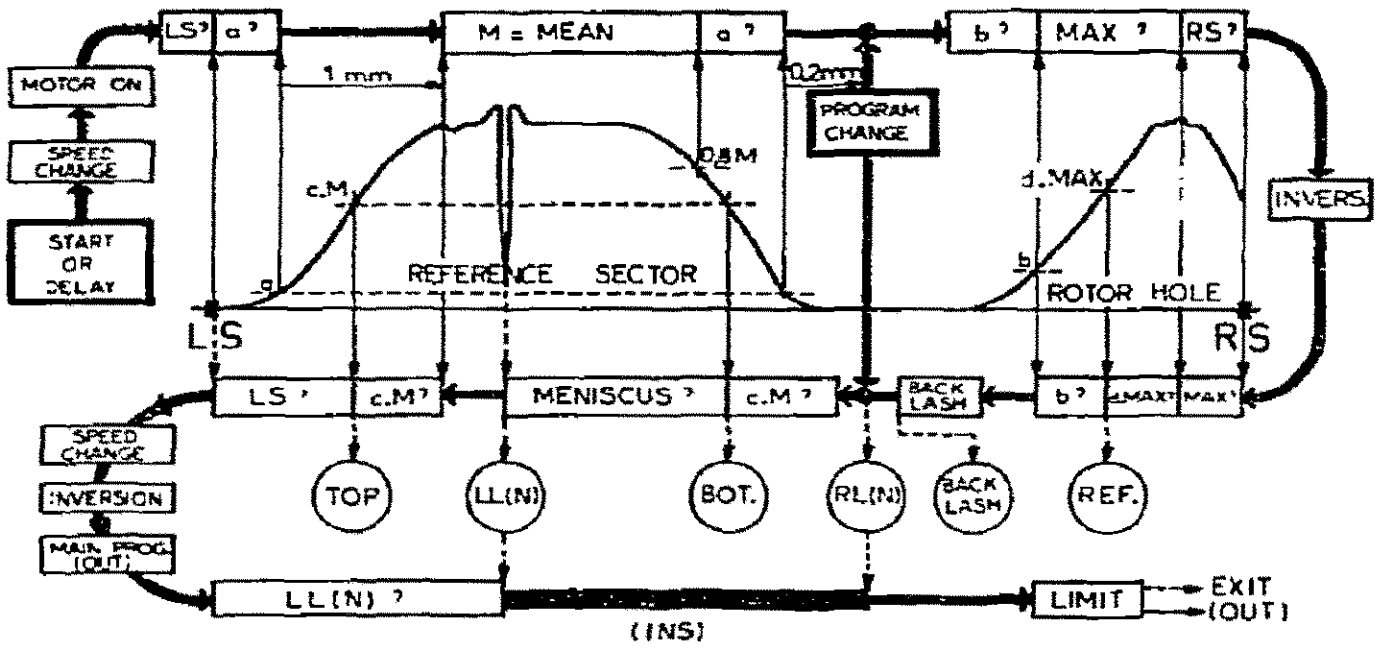


Fig. 4. Initial round-trip organigram. The curve represents very schematically the light intensity as measured by the slit moving along the image. The rise and fall of the light intensity have been strongly exagerated for demonstrative purpose. The program is schematized by the thick line interrupted by the names of the various subprograms (START, MOTOR ON, LS?, RS?, INVERS, C.M.?, LS?,) detailed in section 4.4. Actually, after the initial round trip is completed, the program stops the slit motion and prints (cf. fig. 6) and plots the results before starting the first analysis by SPEED CHANGE, INVERSION, etc. The circles correspond to the parameters measured by MaD and needed for the experiment (positions of the sector top and bottom, the limits, the reference, and the value of the backlash).

so far as the calculation of $\alpha$ is changed. At this time the slit enters the reference hole; here R1 increases very sharply (in a few revolutions) from dark to the maximum light (MAX) coming from the reference hole and eventually, R1 decreases. The MAX value is put in memory; the slit stops at the right stop and reverses its motion now moving to the left. Here, on the way back, the required positions (reference hole, cell bottom, meniscus and cell top) are determined, as well as the backlash of the photomultiplier lead screw.

First R1 is carefully scrutinized until after having passed the MAX position, it reaches the value $d$.MAX corresponding to the reference hole position ($d = \frac{1}{2}$ has been found to be a satisfactory value for defining the reference); the step number and the rotor revolution, for which R1 becomes smaller than $\frac{1}{2}$ MAX, are recorded. Since the number of rotor revolution per step is always recorded, the reference hole position is given as a non integer step number (usually with one decimal place). We achieve a precision of $\pm 3\ \mu$ at the image. Needless to say, if one takes into account the reality of the centrifuge, we do not believe that this precision is very meaningful. Repeating the initial round trip shows that the reference position can actually be known with a precision of about $10\ \mu$ at the cell.

When the slit enters the dark area, the normal program is resumed and $\alpha$ regains its normal value. By carefully scrutinizing the R1 value, MaD then finds the positions (to $\pm$ 0.1 step unit) of the sector bottom (when R1 starts to be greater than $c$.M), of the meniscus (a well defined R1 minimum) and of the sector top (when R1 starts to be smaller than $c$.M). We also adopted $c = \frac{1}{2}$, as we did for $d$. The slit then reaches the left stop and stops; the determined values are printed (in step number, as well as, eventually, in true radical abscissae) along with the other usual information (centrifuge speed, starting time, duration; see fig. 6). The results are then punched and are also always drawn on the digital plotter, from the left to the right stop, one millimeter per radial zone (fig. 5). Log R1 is represented along the vertical axis. Because we have a 12 bit converter, the maximum possible R1 value is 4095. It corresponds to the top of the 30 cm available on the vertical axis. The bottom of the paper corresponds to one hundredth of the maximum, i.e. to R1 = 41. While the single beam R1 distribution is plotted, the special positions (sector top and bottom, left and right limits, reference hole) are indicated by short vertical spikes at their chosen or measured positions.

The plot of the initial round trip is the best possible "vue d'ensemble" and control for the entire experiment protocol. For example, since the experimental maximum R1 value (corresponding to a non absorbing solution) depends, among other things, on the PM high voltage, THT, and on the integrators time constant, ITC, a simple examination of the plot of the initial round trip is enough to see that the experimenter-set choices of THT and ITC are correct. The only other necessary control is an examination of the oscilloscope traces to insure that the light pulses are not saturated. We usually choose the THT so that we get (if the light source permits) a maximum pulse of 7 to 8 volts, and then the ITC is set so as to give a corresponding maximum R1 close to 3500. The clutch (cf. section 3.1) permits one to easily find the position of the R1 maximum along the studied image domain.

Here, during the initial round trip, we measure the backlash of the screw (the rotation of which moves the PM slit along the cell image). When the slit, going to the right, enters the reference, MaD records the exact position (to ± 0.1 step unit) during the sharp rise of R1, for which R1 becomes greater than a fixed value, $b$; on the way back, when the slit leaves the reference hole, MaD again searches the exact position for which R1 becomes smaller than $b$. The difference between these two step numbers is obviously the screw backlash; its value is also printed along with the above data (during the program change, $\beta$ is also changed so that MAX is almost equal to $M$. Hence we adopted for $b$ the value $\frac{1}{2} M$).

The backlash value is taken into account by the RADIAL ABSCISSA subprogram; it was close to 12 steps in 1971, and varied to about 13 steps

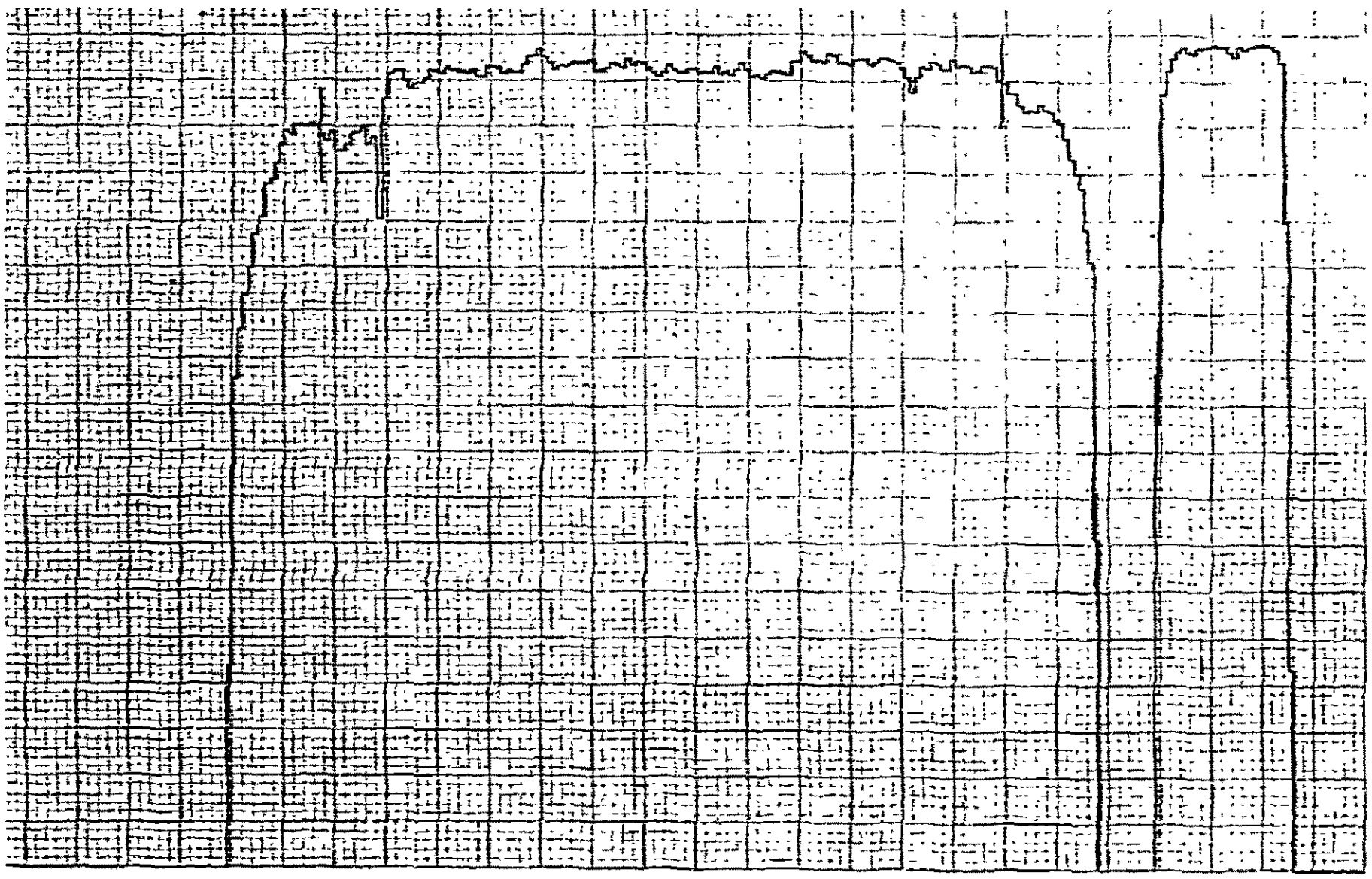

Fig. 5. Initial round trip plot. This corresponds to the experiment of fig. 6. The curve represents the logarithm of the single-beam light intensity distribution of the R1 sector. Along the sharp rises or falls of the light intensities are seen the spikes corresponding to the positions, determined by MaD, of the cell top, the cell bottom and the rotor reference hole. The two spikes visible on the upper part of the figure, correspond to the left and right limits asked for by the experimenter. The distributions are always drawn in such a way that the reference hole position coincides with a full centimeter line of the tracing paper.

by the end of 1974. If the radial resolution has to be better than 8 microns at the cell, only one-way scans must be used since in this case the backlash forbids round trips, but as seen above, such a radial resolution is irrealistic. The backlash was only 2 steps before we added the clutch mechanism to the PM screw system in 1971. It would have been senseless to try to decrease its value since it will never be (or remain for long) smaller than 0.5 step and since MaD handles this problem quite well.

## 5. Communication between MaD and the experimenter

It was shown in section 4 how software and hardware are intimately united during an experiment. The software also plays a major role in the way MaD can be exploited, in its great versatility and also in the presentation of results. All this can be best shown by describing how one starts an experiment. See fig. 6.

It takes 30 seconds for a fast paper tape reader to enter the program into the computer. A colon then appears on the teletype, to which the experimenter should answer. In the case where he is just repeating the previous experiment, it is sufficient to answer with the letter E (for execute) and the experiment starts. Otherwise, the experimenter wishes some or all of a series of questions to be asked; if he wants only one or a few, he just types the question number(s). For example (see below), Q 08 if he wants to change only the left limit.

If he types Q 00, then all the questions are asked, Q 01 and Q 02 being just comments. The answer 4 to Q 03 sets the zone width to 4 steps, i.e. to 4 × 31.25 = 125 $\mu$ at the image (about 80 $\mu$ at the cell). An answer such as 6 to Q 04 means that each analysis should consist of 6 scans, i.e. of 3 round trips, while the answer 20 to Q 05 requires 20 analyses to be made; the time interval between the beginning of each of them is 170 s (answer to Q 06). If the speed differs from 42,000 (Q 07) by more than 1%, then the siren will blast; had the answer been 0, then the speed could be varied at will, the siren blasting only above 70,000 rpm. The answers, in step numbers (250 and 750), to Q 08 and Q 09 are the left and right limits of the radial domain which the experimenter wishes to study. In fact, MaD will impose slightly different limits, 240 and 768 which are multiples of 48 and encompass the

```
: 000
01 EXPERIENCE : DE40.  340 N1
02 VERIFIEZ : CHECK LIST
03 RESOL ISK: 4
04 EXPL/ANA : 6
05 NB ANAL  : 20
06 DT (S)   : 170
07 VITESSE  : 42000
08 LG       : 250
09 LD       : 750
10 AR INIT  : 1
11 NB ECHAN : 2
12 ECH 1    : R1-S2/S1-S2
13 ECH 2    : R2/R1
14 CORR AR  : 0
15 DDO/     : T
16 GRAND    : 1.497
17 CELL (MM): 13.97
18 REF (MM) : 73.12
19 RESULTAT : AP
20 DO H     : 0.400
21 DO B     : -0.100
22 DDO H    : 0.060
23 DDO B    : -0.040
: E
: 030
30 ALPHA (D): 0.3
: E

V=42022  LG=240.0= 57.564 MM  LD=764= 70.556 MM
BAS = 541.2 = 72.114 MM  HAUT = 170.0 = 58.102 MM
REF = 689.4 = 73.120 MM  GRANC = 1.501
DIR = 45.4  DECALAGE VIS = 12.4

V=42022  DEB = 500.6  DUR = 45.8

V=42026  DEB = 670.4  DUR = 45.6

V=42026  DEB = 840.6  DUR = 45.6
```

Fig. 6. Dialogue with MaD. After the questions have been answered (see text), the initial round trip is performed (: E). Four lines are then printed, giving the values determined during the initial round trip. MaD was given (answers to Q 08 and Q 09, see text), in step numbers, the left and right limits (here LG and LD); it measured, again in step number, (see initial round trip section) the positions of the bottom and of the top of the reference sector (here BAS and HAUT), as well as the position of the rotor reference hol (REF). On the other hand, MaD knew the optical magnification (answer to Q 16 : 1.497) and the true radial position of the reference hole (answer to Q 18 : 73.12 mm). This permits the printing of the values of all these positions, both in step numbers and in true radial positions. MaD also knew the length of the reference sector, as measured in a comparator by the experimenter or as determined in previous experiments (answer to Q 17 : 13.97 mm); it could then, from the distance (measured in step number) from the bottom to the top of the sector, calculate the optical magnification (GRANC = 1.501). Since this value was very close to the answer given to Q 16, the experiment went on normally. The speed value (V) is also printed, as well as the backlash (DECALAGE VIS) in step number. MaD then plots the result of the initial round trip (see fig. 5) and, finally, starts the 20 analyses which have been asked for by Q 05. At the completion of each analysis, MaD always prints one line of information: the centrifuge speed (V), the analysis duration (DUR) and the time, in seconds, at which it begun (DEB); then, if it has been requested, the measured absorbancy distribution is plotted.

desired limits. These corrected limits values are then printed after the initial round trip (lower part of fig. 6).

If the answer to Q 08 had been B, MaD would take A, i.e. step 0 (cf. fig. 3), as the left limit; B, answered to Q 09, would set the right limit at Z, i.e. at step 1104. The answer to Q 08 could be also N; in this case, the left limit will be taken as the first step number multiple of 48 immediately to the left of the R1 meniscus whose position has been previously determined by the initial round trip. The response 1 to Q 10 means that the initial round trip will be executed before the first analysis and the important position values printed. If this initial round trip is not wanted, the answer should be 0. The experimenter answers 2 to Q 11 when two absorbancies should be calculated. The answer (R1 − S2)/(S1 − S2) to Q 12, means that the S1 sector absorbancy should be measured, R1 being considered as the reference and S2 as the opaque sector which measures noises and stray light. MaD will then calculate log [(R1 − S2)/(S1 − S2)]; the R1/R2 answer to Q 13 asks for the absorbancy of sector R2 (R1 again being the reference). MaD will then calulate log (R1/R2). If the answer to Q 11 had been 1, then the Q 14 would not have been asked. MaD will thus make alternatively one analysis for the S1 absorbancy radial distribution and one for the R2 distribution. It repeats this cycle ten times to complete the 20 analyses.

To the two questions Q 12 and Q 13, any other combination of the type (R1 − S1)/R2 or R1/S1 or even single beam values such as R1 or R2 − S1, etc. can be answered. It could be possible, if necessary, to follow more than two absorbancy distributions during an experiment. Q 14 is reserved for special controls and is normally answered 0 (cf. also above, condition two).

There are three possible answers to Q 15: 0 would mean that radial distributions of absorbancy (as calculated) are wanted; R would mean that the space derivatives distributions are required, i.e. the differences between adjacent zones; T, which represents one of the most powerful potentialities of MaD, calculates, prints, plots the time differences curves, i.e. the radial distributions of the differences, zone by zone, of the absorbancy values corresponding to two consecutive analyses of the same sample (made, in this case, 340 seconds apart).

When the right answers are given to Q 16 (optical magnification) and to Q 17 (reference hole true radial abscissa at the stated centrifuge speed), then MaD not only knows at all times where the PM slit is, in terms of step number, but also its true radial position in the cell in cm.

When the sector length has been measured on a comparator, its value can be given when Q 18 is asked. This permits (when the initial round trip has been asked for) MaD to calculate the magnification and to check it against the answer given to Q 16 (this calculated magnification is then printed). If there is a serious disagreement (which happens when the lens is not at its correct position along the optical bench) the siren blasts. If the right information is not available, then one abswers 0 to Q 16 and/or A 17 and/or Q 18. If the answers to Q 16 and Q 17 are both 0, then Q 18 is not even asked. Depending on what presentation of the results is wished, the answer to Q 19 can be one or more of the three letters B, P, and T (B = digital plotter, P = paper punch, T = teletype). We always use P because the values of the absorbancies are always punched (in less than 15 seconds), but not the space derivatives or the time differences even if the answer to Q 15 is R or T: this punched tape can then be used later for plotting absorbancies, derivatives or times differences at any desired scale or for printing the values. It is our permanent and very versatile record. We usually do not ask T during the experiment (the teletype is too slow) but most often B is used and the tracing usually takes between 10 and 30 seconds.

By the answers to Q 20 and Q 21, the absorbancy scale on the digital plot is fixed (cf. above). But since, in the chosen example, we asked for time differences curves, another (usually more expanded) scale is requested by Q 22 and Q 23. MaD draws the first analysis normally (absorbancies as measured) with the scale defined by Q 20 and 21. But, starting with the second analysis, it plots only the differences between consecutive analyses of the same sample (with the scale defined by Q 22 and Q 23), etc., and only after the ninth and last difference (corresponding to the tenth analysis), does it draw again, with the first scale, the absorbancies of this last analysis. When, as in the above example, two samples are analyzed, MaD presents these eleven distributions for each sample (the total paper length is then close to 25 feet, but we often use an optional program where all the differences curves corresponding to the same sample are superimposed as in fig. 8).

After Q 23, no more questions appear, the experimenter types E and the experiment starts (actually, E can be typed at any time instead of the answer to any question). Had we not wanted (by Q 19) a digital plot, Q 19 would have been the last question.

Two other questions not normally asked are possible. For example, if after typing E, the oscilloscope shows that, with a new rotor in use, the $\alpha$ (and $\gamma$) gates should be delayed by about $0.3^{\circ}$, one then halts the program, asks for Q 30 and answers + 0.3 before restarting the experiment by E. Similarly, there is a Q 31 question for modifying $\beta$. These two question should be asked when different cell types are used: wider sectors, or single sector cells, etc. Looking at the oscilloscope permits one to very rapidly adjust the $\alpha$ and $\beta$ values corresponding to the new cell.

## 6. Results

The results obtained with MaD will be detailed in the next papers of this series. Nevertheless, it is essential, in this introductory paper, to summarize the important points.

### *6.1. MaD as an absolute photon counter*

We performed a series of experiments which tested the system and helped us to assess MaD characteristics and precision. For these experiments, we prepared a special test program in order to study consecutive pulse values (of R, S or R/S), to print a list of them (up to 512) and to make a statistical analysis. For example, it was easy to determine the standard deviation value of up to 16.384 consecutive R, S or R/S values. On the other hand, by varying the PM slit area, $\mathcal{A}$, (from $4 \times 10^{-4}$ to 10 $mm^2$) and by using two calibrated filters, it was possible to vary the average number of photons per pulse, and hence the average number $\bar{N}$ of photoelectrons per pulse, over a wide range. The PM was not moved. The experiments were performed at 365 nm, the monochromator slit wide open, with a double sector cell, both sectors of which were water filled; the centrifuge was operated at 12,000 rpm.

In the very low light intensity range ($0.03 \leqslant \bar{N} \leqslant 1.3$) where $\mathcal{A}$ was small and the filters were used, R was measured: it was easy to recognize the very constant valued (cf. section 2) noise-alone pulses, to determine their proportion $P_0$, and to verify (with a $\pm 10\%$ precision) that according to the Poisson distribution:

$$P_0 = e^{-\bar{N}} . \tag{1}$$

In the high range ($80 \leqslant \bar{N} \leqslant 2 \times 10^5$), we measured R/S in order to render very small the effect of the residual 50 Hz modulation of the light source; we were able to show that the measured values followed a gaussian distribution. The relative standard deviation, $\sigma$, was given by the Poisson relation (with a $\pm 10\%$ precision):

$$\sigma = (2/\bar{N})^{1/2} \tag{2}$$

The factor 2 arises in this relation because we measure the $\sigma$ of a *ratio* between two equal quantities, $R$ and $S$.

Actually, the experimentally observed relations were in the low range:

$$P_0 = \exp(-k_l \mathcal{A}) , \text{ where } k_l = \text{constant},$$

and in the high range

$$\sigma = (2/k_h \mathcal{A})^{1/2} , \text{ where } k_h = \text{constant}.$$

It was already tempting, in each range, to assume that only if $k\,\mathcal{A} = \bar{N}$ could the corresponding relation be understood. This interpretation was convincingly confirmed when we found that the two differently measured constants $k_l$ and $k_h$ were practically equal (10% difference). Furthermore, taking relations (1) and (2) for granted, it was possible to determine, independently in each range, the pulse value corresponding to one photoelectron. They were almost equal (difference 15%). This then can be considered as a last proof of the validity of (1) and (2).

The average pulse value (i.e. the PM response) was linear from $\mathcal{A} = 4 \times 10^{-4}$ $mm^2$ ($\bar{N} = 80$) to $\mathcal{A} =$ 10 $mm^2$ ($\bar{N} = 2 \times 10^6$). It is this average value which is used for the absorbancy calculations during conventional experiments.

*Note*: with the more than 500 hours-old Xe—Hg light source which we used, at 365 nm, for $\mathcal{A} = 1$ $mm^2$ and at 12,000 rpm, $N \simeq 2 \times 10^5$ for a pulse corresponding to a $2.5^{\circ}$ sector (without a cylindrical lens on the wide open monochromator slit). At 60,000 rpm and 280 nm, with $\mathcal{A} = 0.2$ $mm^2$, $\bar{N} \simeq 200$ for a non-absorbing sample. If the absorbancy is one, then $\bar{N} \simeq 20$.

### 6.2. Precision predictions

There are two main consequences from the previous results. One is the high sensitivity which can be reached (cf. subsection 6.3), the other is the a priori calculation of the precision of a future experiment since the precision depends only on the total number of photoelectrons received by the PM during the scanning of one zone. By taking into account the centrifuge speed, the slit area, the analysis duration, the number of zones in the studied domain and the average number of photoelectrons per slit unit area at the used wavelength, etc., one is able to predict very closely the experimental accuracy for the absorbancy measurements. Usually a comparison is made to a previous experiment. If the scan lasts 25 times longer, then the precision will be improved by a factor of 5. The improvement will be 2 if the slit width is quadrupled or if we use 8-steps zones instead of 2-steps zones. Going from 10,000 to 60,000 rpm leads to the deterioration of the precision by a factor $\sqrt{6}$.

These very simple calculations are made routinely and help us to choose the best protocol. A difference between predicted and observed precision is a diagnosis that something unexpected happened during the experiment or that it was not executed properly.

### 6.3. Some examples of experiments performed with MaD

#### 6.3.1. The fixed radius mode

It is possible to measure the absorbancy of a sample versus time, while the PM slit remains in a fixed position, chosen before the experiment. This, for example, permits one to obtain precise sedimentation coefficient values by measuring the radial dilution effect in the plateau region [14]. In this mode, MaD averages the absorbancy during successive equal time intervals (whose length is given now, in 0.2 s units, as the answer to Q 03); at the end of the experiment, the measured absorbancy values are plotted with 1 mm (along the horizontal axis) per time interval.

In order to perform a fixed radius experiment one starts the program in a slightly different manner and answers only Q 03 (as explained above), Q 20 and Q 21. The experiment can be stopped, at will, by moving a key on the computer console.

The fixed radius type of experiment is one of the most powerful potentialities of MaD.

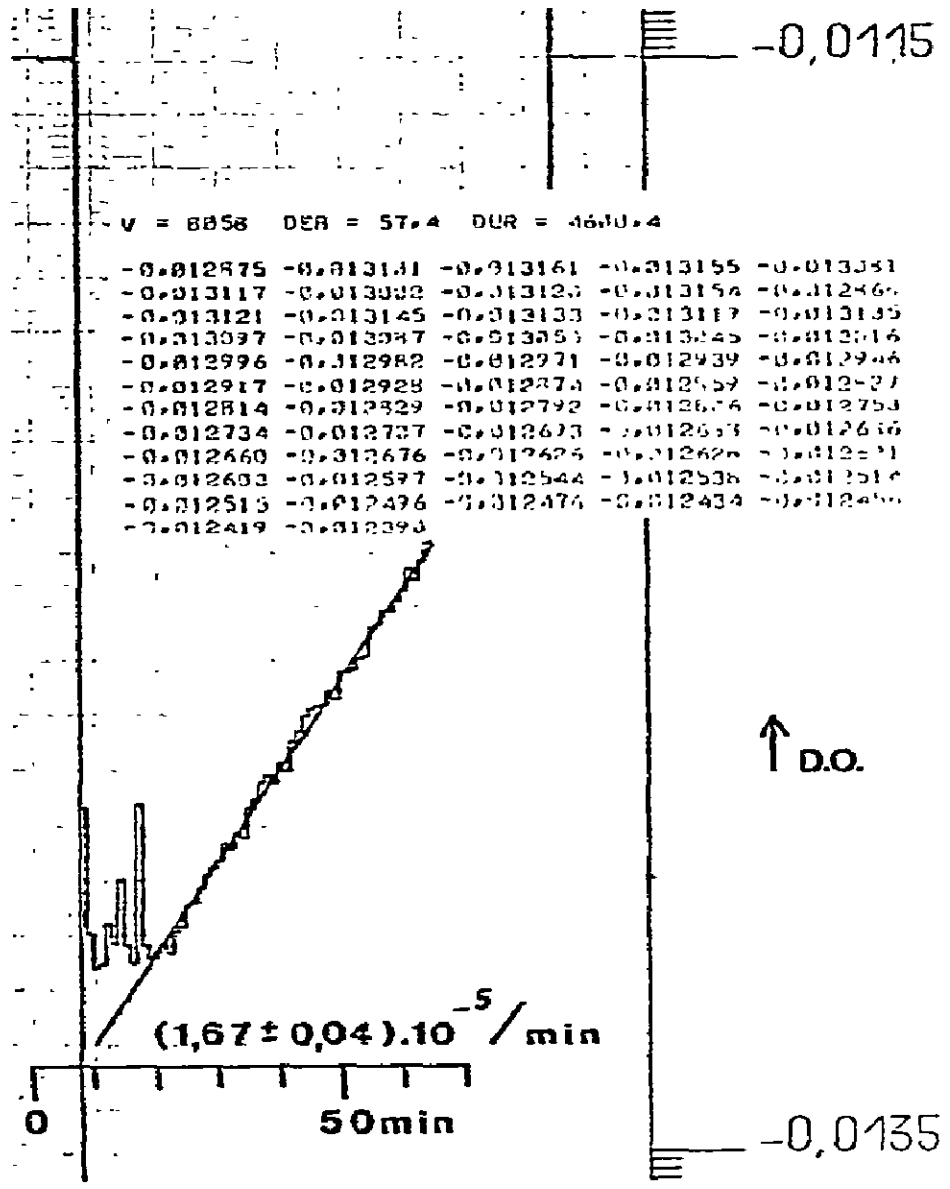


Fig. 7. The ultracentrifuge as a spectrophotometer. A double sector cell was used; both the reference and the sample sectors contained the solution of substrate (here ONPG); at time zero, a known amount of the enzyme $\beta$-galactosidase was added to the sample sector. It was calculated to give, in the centrifuge cell, an activity close to $1.5 \times 10^{-5}$ absorbancy unit/min. The cell was then closed, agitated a few seconds, put in the rotor and spun at 8000 rpm (the sedimentation was thus negligible). The fixed radius mode was adopted and the appearance of the product (ONP) followed at a wavelength of 405 nm. Some supplementary information was added to the plot which resulted from the experiment and the calculated regression line was drawn. The printed values are also shown (D.O. stands for absorbancy). One can see that a few minutes were required for the rotor to stabilize; the standard deviation of the differences between the regression line and the experimental data is close to $6 \times 10^{-6}$ absorbancy units.

#### 6.3.2. MaD as a spectrophotometer

In this case, where the absorbancies are measured

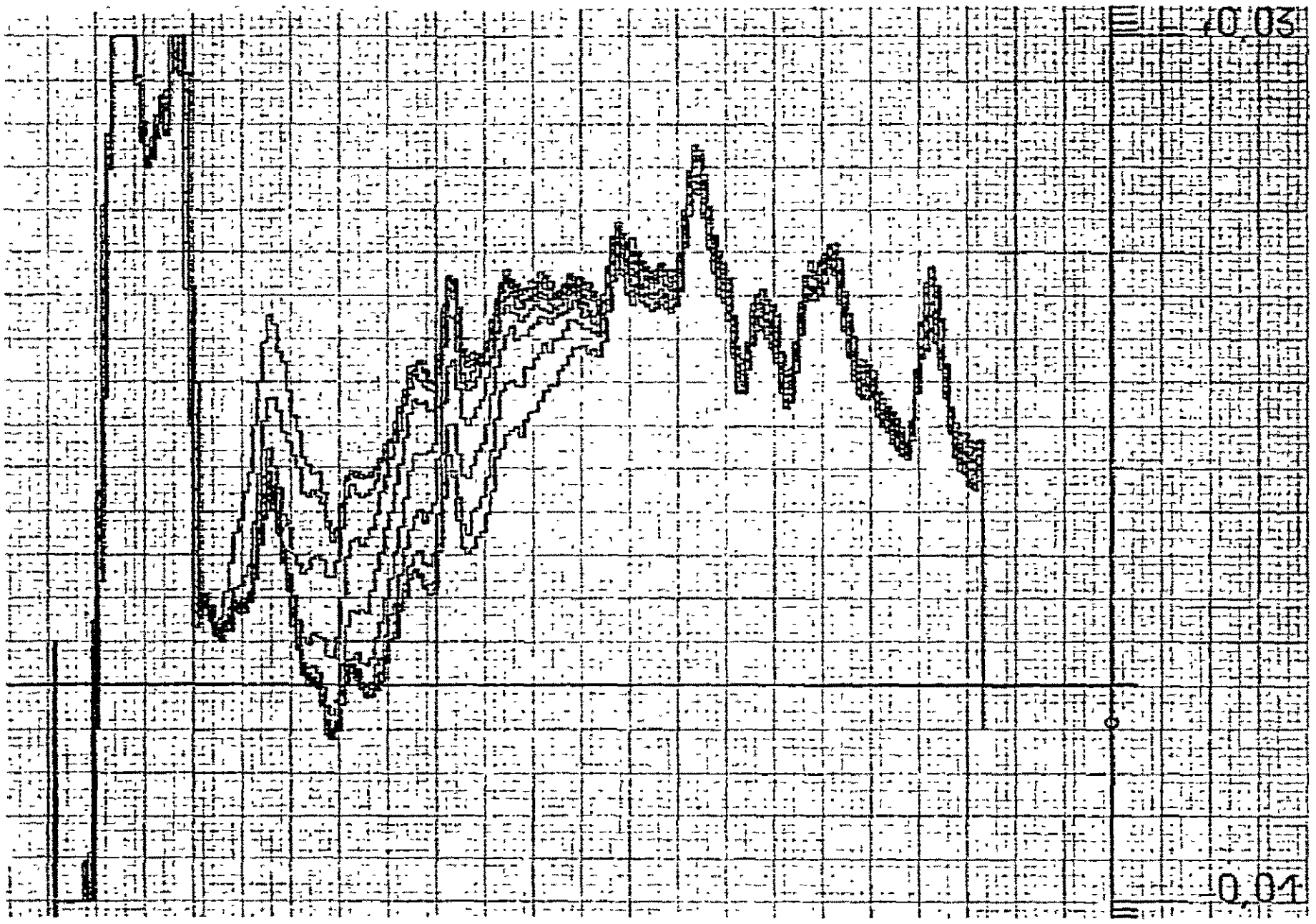


Fig. 8. Boundary sedimentation. A dilute solution of catalase was spun at 44,000 rpm; a 195 sec. round trip analysis was made every 300 sec. The slit width was 0.1 mm and the resolution 4 steps per zone; wavelength 405 nm; temperature close to 23°; 0.1 M phosphate buffer (pH = 7.4). The consecutive absorbancies distributions are superimposed; the first is the upper one. The sample absorbancy (about 0.009) and the base line variations are comparable; it is thus very difficult to directly use such experimental distributions. These true base line variations prevent the use of the space derivative distributions for the determination of the sedimentation coefficient when the sample absorbancy is smaller than about 0.1.

in the fixed radius mode with a $6 \times 10^{-6}$ precision, we made use of an intense line of the Xe—Hg light source, a 10 $mm^2$ slit and a one minute averaging per point. Fig. 7 shows that the intrinsic precision limit of MaD exceeds the normal requirements, in complete agreement with the results of section 6.1.

*6.3.3. Boundary sedimentations*

Fig. 8 shows the base line fluctuations to be $1-3 \times 10^{-3}$ up to $10^{-2}$ absorbancy units. These fluctuations are genuine and correspond to reproducible variations along the cell image. They could correspond to windows or sector shape irregularities (since the integrated $R$ and $S$ signals depend on the sector edges). They often render useless the space derivative curves. These variations almost disappear when the time difference curves are taken into account; the residue can be, as usual, entirely quantitatively accounted for by the Poisson fluctuations of the light source output (fig. 9). From these time differences curves treated as if they schlieren diagrams, one can get a reasonably good (only a few % error) sedimentation coefficient value, $s$. A more precise value can be obtained by a convenient data treatment (to be published).

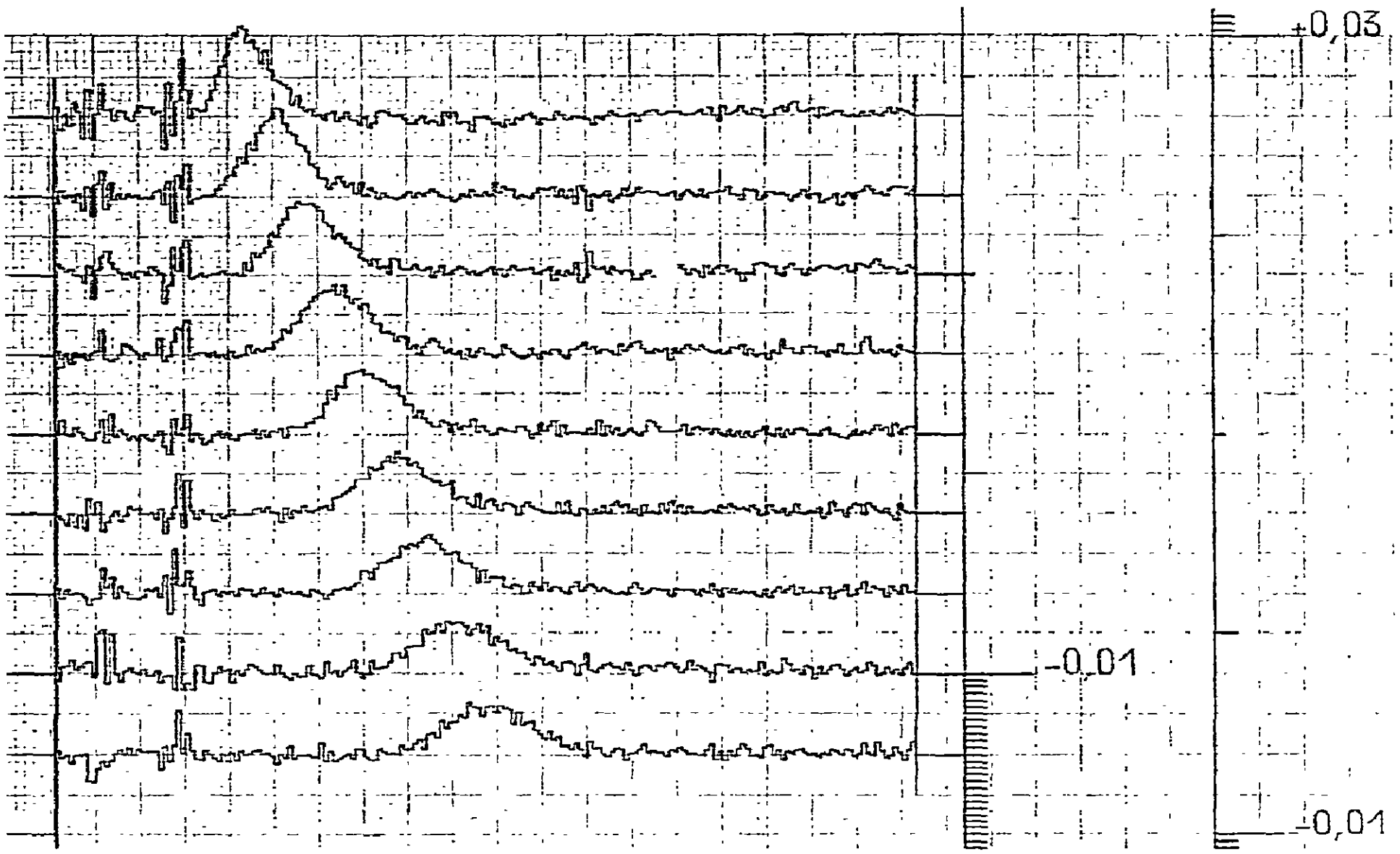


Fig. 9. Boundary sedimentation; the differences curves. The upper curve is the difference between the first and the second absorbancy distributions of figure 8; the pen was then shifted downward for plotting the second differences curve, etc. (the zero-difference level is visible at the left and at the right of each differences curve). The scale on the right shows that it is easy to observe "difference peaks" corresponding to 0.003 absorbancy unit, and that the base line variations visible in fig. 8 are genuine; the residual difference observed (far from the peak) in fig. 9 show that the base line fluctuations are of the order of $2 \times 10^{-4}$ absorbancy units under the experimental conditions of fig. 8. From these curves, $s$ was found to be equal to 11.0 ± 0.2 S (uncorrected).

It is also possible (fig. 10) with the help of a BASIC program (using the MaD computer and plotter) to simulate the time differences curves corresponding to a one (or two independent) species sedimentation experiment (the Faxen–Fujita approximation [9] to the Lamm equation is used), taking into account slit and zone widths, scan duration, round trips, etc. [14] and to compare them with the experimental curves. If the results are not compatible with one or two independent species, the experimental curves should then be compared with simulated curves calculated with the help of the recently evolved correct numerical solution of systems of complete Lamm equations for many interacting particles in the ideal case [10], or even, if necessary, in the concentration dependent case [11], but this requires the help of a computer center.

*6.3.4. Active enzyme centrifugation*

MaD is especially well adapted for this type of work. Indeed it gives, directly, the differences curves from which $s$ is easily deduced [12] and which have been shown to represent fairly well the otherwise invisible active components themselves [13], fig. 11. When working with crude extracts, one has to dilute them at least 50 fold to avoid convection and "sinking" during their layering on top of the substrate solution; the sensitivity of the system allows even very weak activities to be easily picked out.

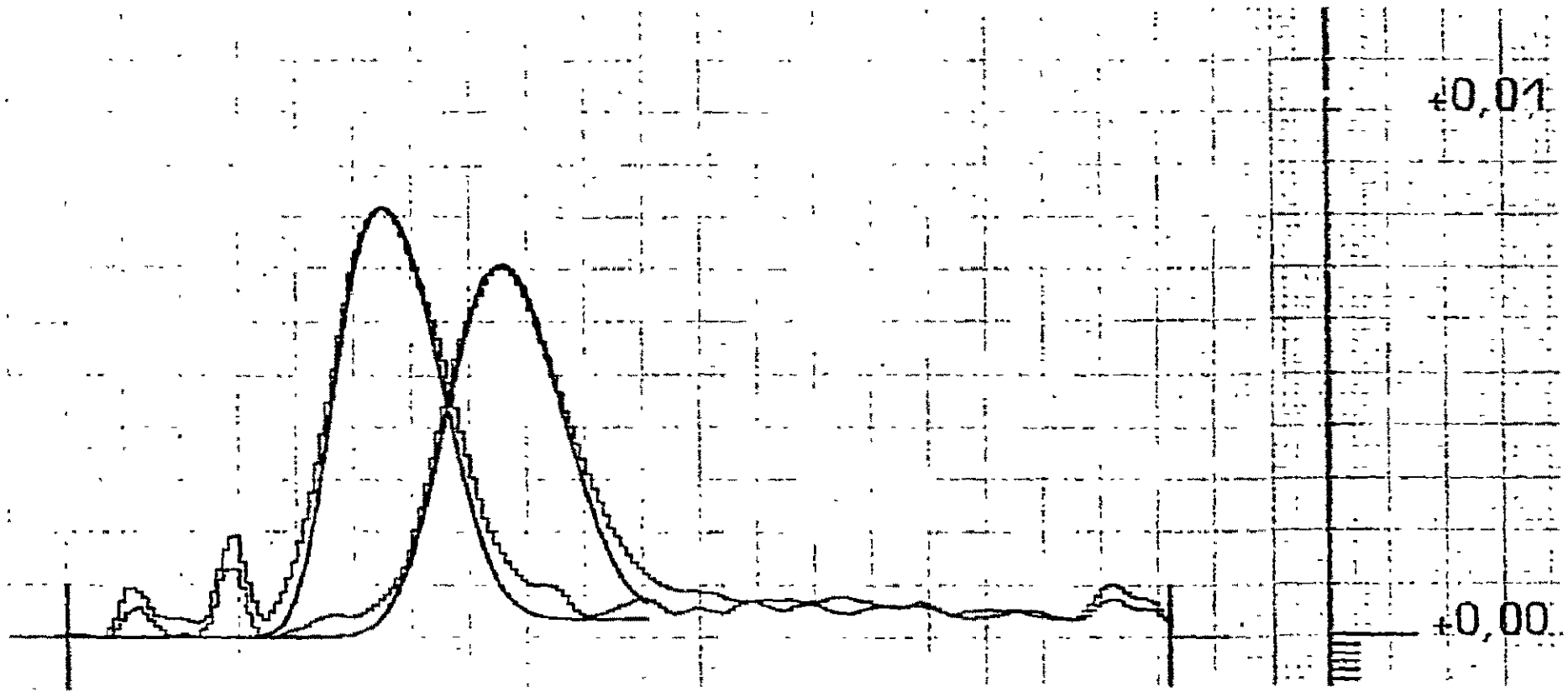


Fig. 10. Experimental versus simulated differences curves. For this figure, the punched tape obtained during the experiment of fig. 8 was used to draw the differences curves between the 5th and the 2nd analysis and then, between the 8th and the 5th. Actually, a moving average (on three consecutive zones) was calculated and plotted. This resulted in slightly smoothed, but otherwise unmodified, differences curves (see text for the $\sigma^*/\sigma$ formula). We then superimposed the corresponding simulated differences curves (using the Faxen–Fujita solution of the Lamm equation, see text), taking into account the speed, the analysis duration, the zone and slit widths, etc.; for these simulated curves we assumed $s = 10.8$ S and $D = 4 \times 10^{-7}$ cm$^2$/s.

## 7. Discussion and conclusions

The fulfillment of all the conditions mentioned in the introduction led to a very convenient system. Its precision far exceeds what was usual previously, not only for ultracentrifuge scanners, but even for bench spectrophotometers. This is entirely due to

a) the integration of whole light pulses
b) the precise and reproducible timing of the gate generation.

Indeed, integration makes use of all the signal and eliminates the systematic but unpredictable error due to the Poisson distribution in the measurement of the maximum of weak light pulse (i.e. giving rise to a small number of photoelectrons at the PM photocathode). Furthermore, since the electronic noise is itself integrated during a constant and very short period, its value is very constant and thus, in practice, does not contribute to the overall experimental error; the latter is entirely due to the Poisson distribution of the number of electron per pulse and can be predicted.

A computer was needed for generating the gates at the right time; but a computer being at hand, it became easy, almost entirely by software, to know the instantaneous position of the PM slit and eventually obtain the versatility, the automation and the convenient results presentation which characterize MaD.

It should be mentioned that in order to reach the same precision as MaD, a photon counter should have a resolution time between pulses at least a hundred times better ($< 50$ picoseconds) than the best currently available instruments (5 nanoseconds). Furthermore, one should realize that to measure a light pulse, a superfast photon counter would need the same number of rotor revolutions as MaD in order to achieve the same precision on its average value.

A laser could be utilized to increase the precision or to decrease the analysis duration; it should be of the continuous type and give a close to 1 mW light power output. Its stability should be better than 0.2% between the two pulses arising from a double sector cell. However, one might wonder about the space charge effect in the PM: it could be so great as to cancel the improved statistical accuracy due to the laser.

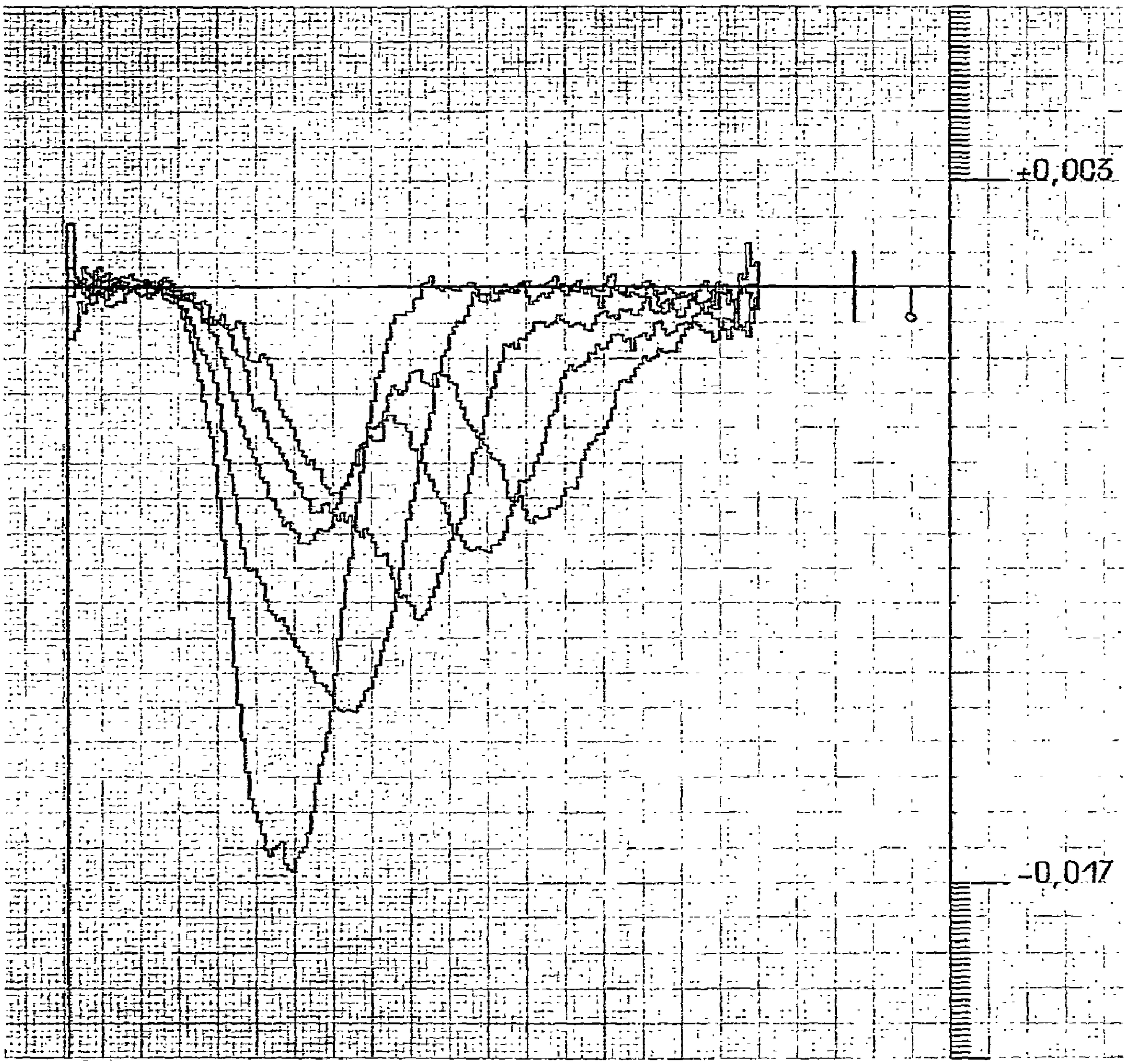


Fig. 11. Active enzyme centrifugation. The figure shows the differences curves obtained during the centrifugation of a crude cell extract of *E. coli Crookes* in which the pyruvate dehydrogenase complex activity was followed [15]. A double sector capillary synthetic-boundary Vinograd-type cell was used. Both sectors contained the reaction substrates (pyruvate, NAD and CoA); during the acceleration, 15 μl of a 300 fold dilution of the cellular crude extract was layered on top on one of the sectors and the NAD → NADH reaction followed at 334 nm. The centrifuge speed was 34000 rpm; analyses were performed every 150 s. For the sake of clarity, only every other differences curve has been drawn. The resolution is 4 steps/zone. The figure shows that the activity is carried by two peaks which are clearly separated although their maximal absorbancies are smaller than 0.007 at the end of the

After a few years of routine works, it appears that among the seven a priori conditions, one, the fifth, could be argued against: the finite duration of a one-way scan and the resulting distortion (cf. condition five) could now be handled easily by comparing experimental and correctly simulated results. But, we have found that the precision is a function of this duration, and that a one hour scan (when the type of experiment permits) is really eight times more precise than a one minute scan (with a correlative eight fold sensitivity increase) and it happens that one hour one-way scans are technically very difficult to perform (minute vibrations of the coded disk during such a slow motion give artefactual ST bit changes). So, for reasons different from the original ones, we still need the round trip technique.

An important but entirely unpredicted characteristic of MaD is the surprisingly good technical behaviour of its hardware. In three years, we have had only two technical failures: a corroded ground connections and a loosed switch. No single component has had to be changed.

In the next paper of this series we will discuss MaD's practically built-in linearity and the almost non-existant zero-offset problem. The use of MaD for equilibrium runs will also be discussed.

The recent advances in the centrifugation theory [10, 13, 11], the introduction of automated and precise scanner systems and of new methodologies in its use [12], should help analytical ultracentrifugation to enter the field of the complex organization of macromolecules in the living cell. Through this new strategy, the analytical ultracentrifuge should regain its important place in biological researches.

## Acknowledgement

We are grateful for the technical assistance provided by Mr. Jean-Claude Deschepper and by Mrs. Annick Larouse. Many discussions with Dr. Roland Van Rapenbusch and Mrs. Marianne Huet, and, in the early part of the work, with Mr. Eamond Kiatipov, were very fruitful. Our thanks are also extended to Mrs. Liliane Corme and Odette Champion for their help in the preparation of the manuscript.

## References

[1] T. Svedberg and H. Rinde, J Am. Chem. Soc. 46 (1924) 2677.
[2] R. Cohen, Compte rendu de fin de contrat 68-01-307 (1971) 36 pages (D.G.R.S.T. 35, rue St-Dominique, 75007. Paris).
[3] US. Patent 3.712. 742 (1973).
[4] H.K. Schachman and S.J. Edelstein, in: Methods in Enzymology, vol. XXVII, eds. C.H.W. Hirs and S.N. Timasheff (Academic Press, New-York and London, 1973) p. 3.
[5] H.K. Schachman, in: Ultracentrifugal Analysis in Theory and Experiment, ed. J.W. Williams (Academic Press, New-York and London, 1963) p. 173.
[6] K. Lamers, F. Putney, I.Z. Steinberg and H.K. Schachman, Arch. Biochem. Bioph., 103 (1963) see p. 399.
[7] W.F. Sheppard, Proc. Lond. Math. Soc. 29 (1898) 353.
[8] R. Cohen, in: Techniques de Laboratoire, I, 2, ed. J. Loiseleur (Masson, Paris, 1963), see p. 876.
[9] H. Fujita, Mathematical Theory of Sedimentation Analysis, (Academic Press, New-York and London, 1952).
[10] J.M. Claverie, H. Dreux and R. Cohen, Biopolymers 14 (1975) 1685.
[11] J.M. Claverie, submitted to Biopolymers.
[12] R. Cohen and M. Mire, Eur. J. Biochem. 23 (1971) 267.
[13] R. Cohen and J.M. Claverie, Biopolymers 14 (1975) 1701.
[14] R. Cohen, unpublished results.
[15] B. Schmitt, unpublished results.